

## Evaluation of Drilling Process for Clamped-Free-Clamped-Free Rectangular Plate Using Vibration Analysis

Dr. Mauwafak Ali Tawfik\* & Sami Ali Nama 

Received on:9/2/2010

Accepted on:5/1/2011

### Abstract

In this paper, the superposition method was used to obtain the solution for the forced vibration of clamped-free-clamped-free (CFCF) isotropic rectangular plates subjected to a concentrated drilling force. This method was found to work extremely well, and fewer terms in the series were used to provide an equivalent accuracy of solutions. The drilling force signals can be represented by Fourier series; the terms of the series were used to calculate the plate dynamic response at any point on the plate surface. The effect of the drilling conditions on Fourier series terms was analyzed and an empirical equation was derived to calculate the fundamental Fourier frequency at different drilling conditions. It was found that the speed and feed have pronounced effects on the Fourier fundamental frequency term.

### تقييم عملية تثقيب الصفائح باستخدام تحليل الاهتزاز

#### الخلاصة

استخدمت طريقة التراكب في هذا البحث للحصول على حل الاهتزاز القسري للصفحة المتجانسة، الرقيقة، مربعة الشكل مثبتة من جانبيين متقابلين وحررة الحركة من الجانبين الآخرين ومعرضة لقوة التثقيب. وقد وجد إن طريقة التراكب تعمل بشكل جيد من خلال استخدام حدود قليلة من سلسلة فوريير للحصول على نتائج دقيقة ومقبولة للحل، حيث استخدمت حدود السلسلة لحساب الاستجابة الديناميكية للصفحة عند أي نقطة على سطح الصفحة. تم تحليل تأثير ظروف التثقيب على حدود سلسلة فوريير وتم إيجاد معادلة تطبيقية تجريبية لحساب التردد الأساس لسلسلة فوريير عند ظروف تثقيب مختلفة. وقد وجد ان تأثير السرعة الدورانية ومعدل التغذية واضحا على حد التردد الأساسي لسلسلة فوريير.

### Introduction

The cutting forces are the main reason of the problems related to drilling in manufacturing, such as form and surface errors, tool wear, and vibration. Models for drilling thrust force and torque had been mainly investigated for the standard conical-point twist drill.

The superposition method is an efficient approach; it was used by Gorman [1] for the free vibration of

rectangular plates. The method is unique in that the governing differential equation is satisfied exactly throughout the domain of the plate and the boundary conditions are satisfied to any desired degree of accuracy. In addition, only a limited number of terms need be used to ensure convergence of the solution.

In this paper, the technique is employed for the problem of forced vibration of the clamped-free-

\* Machines & Equipments Engineering Department, University of Technology/ Baghdad

\*\* Foundation of Technical Education/ Baghdad

clamped-free isotropic rectangular plate subjected to a concentrated drilling force acting at any point on the plate surface.

Donaldson [2] presented an approximate method of analysis for the response of a thin plate subjected to a single frequency, forced harmonic vibration, and provided numerical results in reference [3]. Laura and Duran [4] studied the response and bending moments of a vibrating thin elastic rectangular plate, which is clamped along the boundary and subjected to a uniformly distributed sinusoidal excitation force. Wu [5] studied the dynamic characteristics of a rectangular plate undergoing forces moving along a circular path using the finite element method. It was concluded that, the rotating speed and the forcing frequency are the two key factors affecting the dynamic responses of the rectangular plate. Chern and Lee [6] investigated the effects of the assisted vibration on the drilling quality of an aluminum alloy and a structural steel, while Chang and Bone [7] proposed a thrust force model for the vibration assisted drilling of aluminum.

Analytical procedure

The dimensionless governing differential equation for the forced vibration of an isotropic rectangular plate,

$$\frac{\partial^4 w(\xi, \eta)}{\partial \eta^4} + 2\phi^2 \frac{\partial^4 w(\xi, \eta)}{\partial \eta^2 \partial \xi^2} + \phi^4 \frac{\partial^4 w(\xi, \eta)}{\partial \xi^4} - \phi^4 \lambda^4 w(\xi, \eta) = \frac{b^4 P(\xi, \eta)}{D} \dots (1)$$

In order to obtain the solution for the forced Clamped-Free-Clamped-Free plate, five plates were considered with simpler boundary

conditions which can be handled by Levy-solution (these plates will be called “building blocks“ ). The solution obtained for each of these plates will be superposed such that equation (1) and the boundary conditions of the actual plate are completely satisfied.

The first and third building blocks shown on the right side of figure (1) are driven along one edge by a distributed harmonic slope, while the second and fourth building blocks are driven along one edge by a distributed harmonic bending moment, and the fifth block is subjected to a concentrated drilling force at the dimensionless co-ordinate (u, v).

The solution for the first building block is taken in the Levy-type form:

$$W_1(\xi, \eta) = \sum_{m=1,2,3}^{\infty} Y_m(\eta) \sin(m\pi\xi) \dots (2)$$

Substituting this solution into equation (1) and noticing that P=0, yields:

$$Y_m''''(\eta) - 2(\phi m \pi)^2 Y_m''(\eta) + (\phi m \pi)^4 Y_m(\eta) - \phi^4 \lambda^4 Y_m(\eta) = 0 \dots (3)$$

The solution for equation (3) is:

For  $\lambda^2 > (m\pi)^2$

$$Y_m(\eta) = A_m \cosh(\beta\eta) + B_m \sinh(\beta\eta) + C_m \sin(\gamma\eta) + D_m \cos(\gamma\eta) \dots (4)$$

For  $\lambda^2 < (m\pi)^2$

$$Y_m(\eta) = A_m \cosh(\beta\eta) + B_m \sinh(\beta\eta) + C_m \sinh(\gamma\eta) + D_m \cosh(\gamma\eta) \dots (5)$$

where  $\beta = \phi \sqrt{\lambda^2 + (m\pi)^2}$  and  $\gamma = \phi \sqrt{\lambda^2 - (m\pi)^2}$  or

$$\lambda = \phi \sqrt{(m\pi)^2 - \lambda^2}$$

whichever is real

The undetermined coefficients in the case solutions are defined by enforcing the boundary conditions at  $\eta = 0$  and  $\eta = 1$

The boundary conditions for the slip shear edge at  $\eta = 0$  are:

$$\sum_{m=1,2,3}^{\infty} Y_m'(0) \sin(m\pi\xi) = 0$$

$$\sum_{m=1,2,3}^{\infty} Y_m'''(0) \sin(m\pi\xi) = 0 \quad \dots(6)$$

The boundary conditions for the zero shear force edge at  $\eta = 1$  are:

$$\frac{\partial w(\xi, \eta)}{\partial \eta} = \sum_{m=1,2,3}^{\infty} E_m \sin(m\pi\xi),$$

$$\frac{\partial^3 w(\xi, \eta)}{\partial \eta^3} + (2 - \mu)\phi^2 \frac{\partial^3 w(\xi, \eta)}{\partial \eta \partial \xi^2} = \dots(7)$$

where  $E_m$  is the distributed harmonic slope function.

The final solution can be obtained for the first building block as follows:

For  $\lambda^2 > (m\pi)^2$

$$Y_m(\eta) = E_m \left\{ \frac{\gamma^2 + (2 - \mu)\phi^2(m\pi)^2}{\beta(\beta^2 + \gamma^2)\sinh\beta} \right\} \cosh(\beta\eta)$$

$$- E_m \left\{ \frac{\beta^2 - (2 - \mu)\phi^2(m\pi)^2}{\gamma(\beta^2 + \gamma^2)\sin\gamma} \right\} \cos(\gamma\eta) \dots(8)$$

For  $\lambda^2 < (m\pi)^2$

$$Y_m(\eta) = E_m \left\{ \frac{(2 - \mu)\phi^2(m\pi)^2 - \gamma^2}{\beta(\beta^2 - \gamma^2)\sinh\beta} \right\} \cosh(\beta\eta) +$$

$$E_m \left\{ \frac{\beta^2 - (2 - \mu)\phi^2(m\pi)^2}{\gamma(\beta^2 - \gamma^2)\sin\gamma} \right\} \cosh(\gamma\eta) \dots(9)$$

For the second building block, edge  $\xi=1$  have zero displacement edge conditions

$$w(\xi, \eta) = 0,$$

$$- \frac{D}{a} \left[ \frac{\partial^2 w(\xi, \eta)}{\partial \xi^2} + \frac{\mu}{\phi^2} \frac{\partial^2 w(\xi, \eta)}{\partial \eta^2} \right]$$

$$= \sum_{n=0,1,2}^{\infty} E_n \cos(n\pi\eta) \dots(10)$$

The following solution can be obtained

For  $\lambda^2 \phi^2 > (n\pi)^2$

$$Y_n(\xi) = \frac{E_n}{(\beta^2 + \gamma^2)\sinh(\beta)} \sinh(\beta\xi) - \frac{E_n}{(\beta^2 + \gamma^2)\sin(\gamma)} \sin(\gamma\xi) \dots(11)$$

For  $\lambda^2 \phi^2 < (n\pi)^2$

$$Y_n(\xi) = \frac{E_n}{(\beta^2 - \gamma^2)\sinh(\beta)} \sinh(\beta\xi) - \frac{E_n}{(\beta^2 - \gamma^2)\sin(\gamma)} \sin(\gamma\xi) \dots(12)$$

Solution for the third and fourth building blocks can be derived from the first and second building blocks, by simply replacing the coordinates  $\eta$  and  $\xi$  by  $(1-\eta)$  and  $(1-\xi)$  respectively.

The solution for the fifth building block can be obtained by the method as described in reference [8].

For  $\lambda^2 > (m\pi)^2$

For  $\eta < v$

$$w(\xi, \eta) = \frac{Pb^3}{aD\phi^2\lambda^2}$$

$$\sum_{m=1}^L \left\{ \sin(m\pi u) \left\{ \frac{\sin(\gamma(1-v))\sin(\gamma\eta)}{\gamma\sin(\gamma)} - \frac{\sinh(\beta(1-v))\sinh(\beta\eta)}{\beta\sinh(\beta)} \right\} \right\} \sin(m\pi\xi) \dots(13)$$

For  $\eta \geq v$

$$w(\xi, \eta) = \frac{Pb^3}{aD \phi^2 \lambda^2} \sum_{m=1}^L \left\{ \sin \left( \frac{m \pi}{u} \right) \left[ \frac{\sin(\gamma(1-v)) \sin(\gamma \eta)}{\gamma \sin(\gamma)} - \frac{\sinh(\beta(1-v)) \sinh(\beta \eta)}{\beta \sinh(\beta)} + \frac{\gamma \sinh(\beta(\eta-v))}{\gamma \beta} - \frac{\beta \sin(\gamma(\eta-v))}{\gamma \beta} \right] \right\} \sin(m \pi \xi) \dots \dots \dots (14)$$

For  $\lambda^2 < (m\pi)^2$   
 For  $\eta < v$

$$w(\xi, \eta) = \frac{Pb^3}{aD \phi^2 \lambda^2} \sum_{m=L}^{\infty} \left\{ \sin(m \pi u) \left[ \frac{\sinh(\gamma(1-v)) \sinh(\gamma \eta)}{\gamma \sinh(\gamma)} - \frac{\sinh(\beta(1-v)) \sinh(\beta \eta)}{\beta \sinh(\beta)} \right] \right\} \sin(m \pi \xi) \dots \dots \dots (15)$$

For  $\eta \geq v$

$$w(\xi, \eta) = \frac{Pb^3}{aD \phi^2 \lambda^2} \sum_{m=L}^{\infty} \left\{ \sin(m \pi u) \left[ \frac{\sinh(\gamma(1-v)) \sinh(\gamma \eta)}{\gamma \sinh(\gamma)} - \frac{\sinh(\beta(1-v)) \sinh(\beta \eta)}{\beta \sinh(\beta)} + \frac{\gamma \sinh(\beta(\eta-v))}{\gamma \beta} - \frac{\beta \sinh(\gamma(\eta-v))}{\gamma \beta} \right] \right\} \sin(m \pi \xi) \dots \dots \dots (16)$$

The CFCF plate superimposed solution will be the summation of the solutions of the five building blocks, and it must satisfy the prescribed boundary conditions of the original plate, which requires that the net

slope along edges  $\xi=0$  and  $\xi=1$ , and the bending moment along edges  $\eta=0$  and  $\eta=1$  must be zero. This is realized by expanding the contributions of each building block toward the slope and bending moment along the four edges in trigonometric series, and enforcing the net Fourier coefficients of each term to equal zero. The result is a set of 4K simultaneous non-homogeneous algebraic equations relating the coefficients,  $E_m$ ,  $E_n$  etc and P, where K is the number of terms used in the building block solutions. The solution for the set of equations can be obtained by a computer program.

Experimental Work

The purpose of the experimental part is to study the vibration phenomena of a (Clamped-Free-Clamped-Free) thin rectangular plate during the drilling operation, to do so; a clamping arrangement was designed and built. The experimental setup enables us to pick up the drilling force and acceleration signals. The setup, hence, consist of a piezoelectric force transducer (Model 201B03), accelerometer (KISTLER Model 8276A5), DVA meter (Ling Dynamic Systems Sr. No. 455), and FFT analyzer (YOKOGAWA Model DL 1620). Figure (2) shows the layout of the experimental setup, while figure (3) shows the accelerometer and force transducer mounting.

A Pacmill model 3KS milling machine was used to accomplish the experimental work due to its capability to perform drilling operation in addition to the milling process. It has a spindle speed range (70 to 4620 rpm) with feed rates (0.04, 0.08, and 0.15 mm/rev).

Standard HSS twist drill was used to perform the drilling operation. The

specifications of the drill angles were: 115° point angle, 25° helix angle and 135° chisel edge angle. Four different drill diameters were used: 4, 5, 6 and 7 mm. For all the experiment, drilling was at the center of the plate.

Four different experimental investigations were performed as follows:

Drilling with different spindle speeds (800, 1300, 1600, and 1810 RPM), different spindle feed rates (0.04, 0.08, and 0.15 mm/rev), different drill diameters (4, 5, 6, and 7 mm), and different thicknesses (2, 3, 4, and 5mm).

#### Results and Discussions Analyzing the thrust force signals.

The force results obtained experimentally can be analyzed analytically by the help of Fourier series which can be written as [9]:

$$F(t) = \frac{a_0}{2} + \sum_{n=1}^{\infty} \left( A_n \cos(n\omega t) + B_n \sin(n\omega t) \right) \quad (17)$$

Where  $F(t)$  is the force function (N),

$\omega = \frac{2\pi}{T}$  is the fundamental

frequency (rad/sec), T period (sec) and  $a_0, A_1, A_2, \dots, B_1, B_2, \dots$  are constant coefficients. Figure (4) shows the force signal obtained during the drilling operation. Find Graph software [10] was used to analyze the experimental force signals to obtain the function that represents the thrust force as a Fourier series.

#### Fourier series factors analysis.

The main factors in Fourier series are the time, Fourier fundamental frequency, and amplitude. The drilling force is affected by the drilling conditions, so when the drilling force is represented by Fourier series, each of these factors is

affected by the different cutting conditions.

The Fourier fundamental frequency is of importance as its value (or its multiplies) that may coincide with the natural frequency of the plate and this in turn leads to the resonance. ( $\omega$ ) increases rapidly as the rotational drill speed and drill feed increase as shown in figures (5) and (6), respectively; while it decreases slightly as the drill diameter and plate thickness increase as shown in figures (7) and (8). It can be concluded that increasing of speed or feed rate may cause the Fourier fundamental frequency to coincide with the natural frequency of the plate in a manner faster than changing the drill diameter or plate thickness. Increasing both of the speed and feed rate at the same time results in more effect than increasing each one individually.

#### Fundamental Fourier frequency ( $\omega$ ) model.

To find the relation between the Fourier fundamental frequency ( $\omega$ ) and the drilling variables, DataFit software [11] was used to analyze ( $\omega$ ) as a function in terms of the different drilling variables obtained experimentally. Six fitting models were used to represent this relation. For each model, the Fourier fundamental frequency ( $\omega$ ) was calculated for the different drilling conditions and the results were compared with that experimentally obtained. The percentage error between the theoretical and experimental ( $\omega$ ) was calculated as shown in table (1). Model (1) was chosen because it has the minimum percentage error range. The relation between the Fourier fundamental frequency ( $\omega$ ) and the drilling variables can be written as:

$$\omega = \frac{N^{0.44} * f^{0.295}}{D_d^{0.141} * h^{0.072}} - 6.132 \quad (rad/sec)$$

.....(18)

The ANSYS software was used to study the free vibration and determine the first three resonance limits for different plate dimensions, the results are listed in table (2).

For a certain drilling conditions, the proposed model was used to determine the value of ( $\omega$ ), results are listed in table (3). For the CFCF plate, as ( $\omega$ ) is known, figures (9), (10) and (11) can be used to determine the allowed maximum plate lateral dimensions before reaching the resonance limit and from which the limit of the drilling conditions may be deduced. If the plate lateral dimensions are known, the value of ( $\omega$ ) can be determined from the curve for a given natural frequency, and then the allowable drilling conditions can be optimized within this range of ( $\omega$ ) to avoid the vibration at resonance.

**Conclusions**

Fourier series can be effectively used to represent and analyze the behavior of the drilling force and can be related to the drilling conditions. Increasing the speed and feed rate increases rapidly the ( $\omega$ ) term in Fourier series, while increasing the drill diameter or plate thickness decreases slightly the ( $\omega$ ) term. The Fourier fundamental frequency term ( $\omega$ ) can be used to determine the allowable maximum lateral dimensions of the plate to be drilled to avoid the resonance limits.

**References**

[1]D. J. Gorman, "Free vibration analysis of rectangular plates",

New York, Elsevier, North Holland, 1982.

[2]B. K. Donaldson, "A new approach to the forced vibration of thin plates ", J. Sound and Vibration, Vol. 30, pp. 397-417, 1973.

[3] B. K. Donaldson and S. Chander, "Numerical results for extended field method application", J. Sound and Vibration, Vol. 30, pp. 437-444, 1973.

[4]P. A. A. Laura and R. Duran, "A note on forced vibration of a clamped rectangular plate", J. Sound and Vibration, Vol. 42, pp. 129-135, 1975.

[5]Jia-Jang Wu, "Vibration of a rectangular plate undergoing forces moving along a circular path", Finite elements in analysis and design, Vol. 40, pp. 41-60, 2003.

[6]Gwo-Liang Chern, and Han-Jou Lee "Using workpiece vibration cutting for micro-drilling", Int. J. Adv. Manuf. Technol., Vol.27, pp688-692, 2006.

[7]S. S. F. Chang, and G. M. Bone, "Thrust force model for vibration assisted drilling of aluminum 6061-T6", Int. J. Mach. Tool Manufact., Vol. 49, pp. 1070-1076, 2009.

[8]D. Zhou, and T. Ji, "Free vibration of rectangular plates with internal column support", J. Sound and Vibration, Vol. 297, pp. 146-166, 2006.

[9]V. P. Singh, "Mechanical vibrations", DHANPAT & Co., India, 3<sup>rd</sup> ed, 2004.

[10]FindGraph software, Version 2.005, Uniphiz lab, 2008.

[11] DataFit software, Version 9.0.59, Oakdale Engineering, 2008.	N	Drill rotational speed (rpm)
Appendix: Nomenclature	$w(\xi, \eta)$	Amplitude of plate lateral displacement
a, b	$\xi = x/a$ , $\eta = y/b$	Plate lateral dimension (mm) Plate spatial coordinates
D	$\phi = b/a$	Plate flexural rigidity (N.m) Plate aspect ratio
$D_d$	$\lambda^2 = \omega^2 a^2 \sqrt{\rho h / D}$	Drill diameter (mm) Plate eigenvalue
f	P	Drill feed rate (mm/rev) Amplitude of applied force (N)
h	$\mu$	Plate thickness (mm) Poisson's ratio for the plate material

Table (1) comparison between different models to calculate ( $\omega$ ).

	Model	% Error range
1	$\omega = N^a * f^b * D_d^c * h^d + e$	0.0468 ~ 12.204
2	$\omega = a * N^b * f^c * D_d^d * h^e$	0.364 ~ 13.997
3	$\omega = a * N + b * f + c * D_d + d * h + e$	0.291 ~ 13.308
4	$\omega = \text{Exp} (a * N + b * f + c * D_d + d * h + e)$	0.656 ~ 31.563
5	$\omega = a * N + b * f + c * D_d + d * h$	0.598 ~ 37.565
6	$\omega = N^a * f^b * D_d^c * h^d$	2.646 ~ 54.864

( $\omega$ =Fourier fundamental frequency, N=RPM, f=feed,  $D_d$ =drill diameter, h=thickness)

**Table (2) First three resonance limits for different plate dimensions.**

Plate length (m)	Plate thickness								
	1 mm			2 mm			3 mm		
	$\omega_1$	$\omega_2$	$\omega_3$	$\omega_1$	$\omega_2$	$\omega_3$	$\omega_1$	$\omega_2$	$\omega_3$
0.25	89.205	105.8	174.66	178.41	211.6	349.32	267.61	317.41	523.98
0.30	61.948	73.474	121.29	123.9	146.95	242.58	185.84	220.42	363.87
0.35	45.513	53.981	89.112	91.025	107.96	178.22	136.54	161.94	267.34
0.4	34.846	41.329	68.226	69.691	82.658	136.45	104.54	123.99	204.68
0.45	27.532	32.655	53.907	55.065	65.31	107.81	82.597	97.965	161.72
0.50	22.301	26.451	43.665	44.602	52.901	87.33	66.903	79.352	130.99
0.75	9.9116	11.756	19.407	19.823	23.512	38.813	29.735	35.267	58.22

**Table (3) Variation of theoretical ( $\omega$ ) with maximum plate length. (plate thickness = 1 mm)**

Speed (rpm)	Feed (mm/rev)	Diameter (mm)	$\omega_1$ (rad/sec)	Plate length (mm)	$\omega_2$ (rad/sec)	$\omega_3$ (rad/sec)
4600	0.15	5	12.558	0.666	14.909	24.612
4620	0.20	5	14.255	0.626	16.875	27.858
4620	0.25	4	16.34	0.584	19.389	32.009
5000	0.25	4	17.137	0.570	20.354	33.601

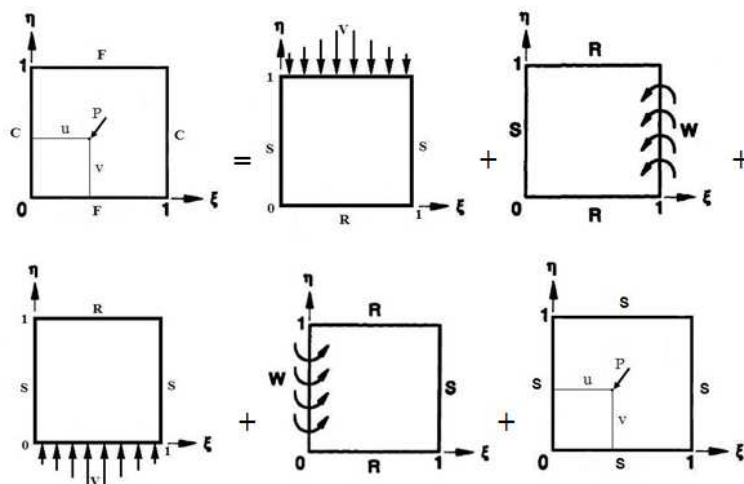


**Figure (1) Building blocks for the forced vibration of CFCF plates.**

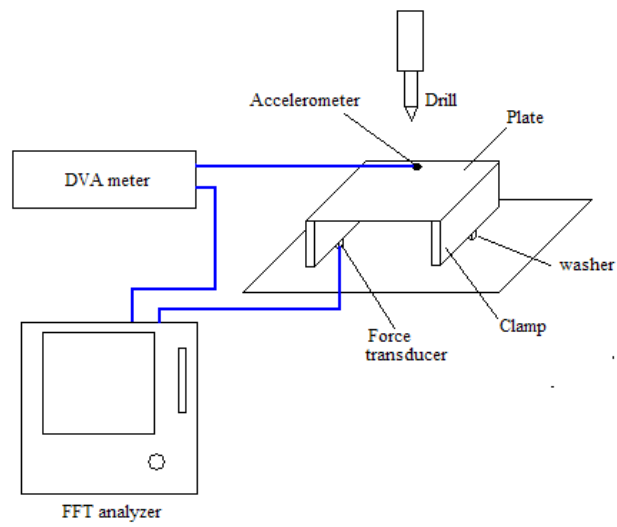


Figure (2) The layout of the experimental setup

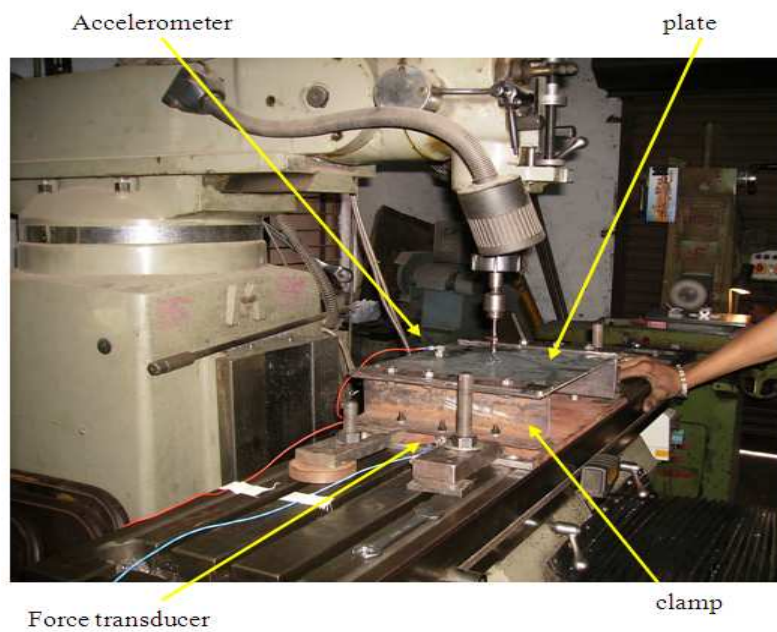
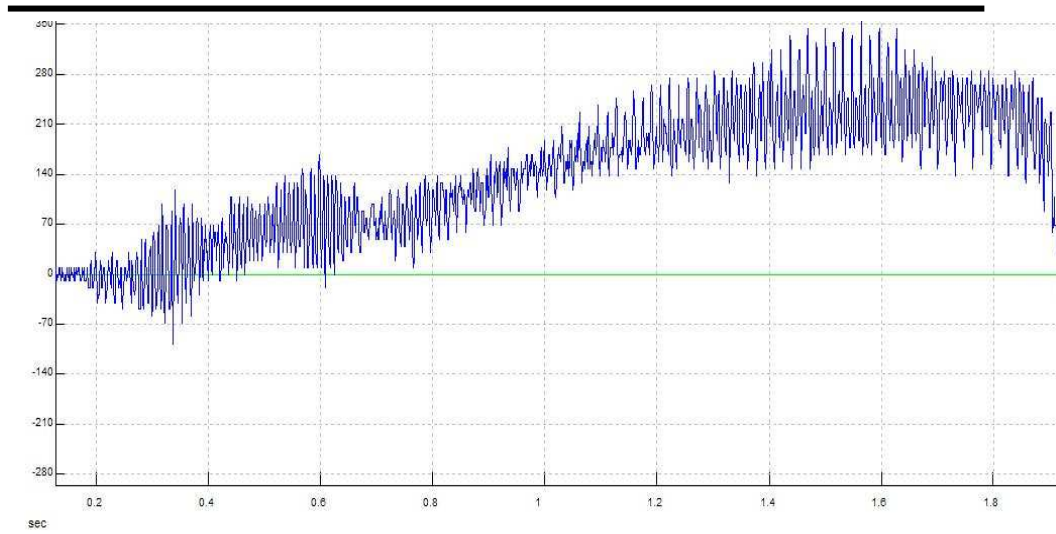
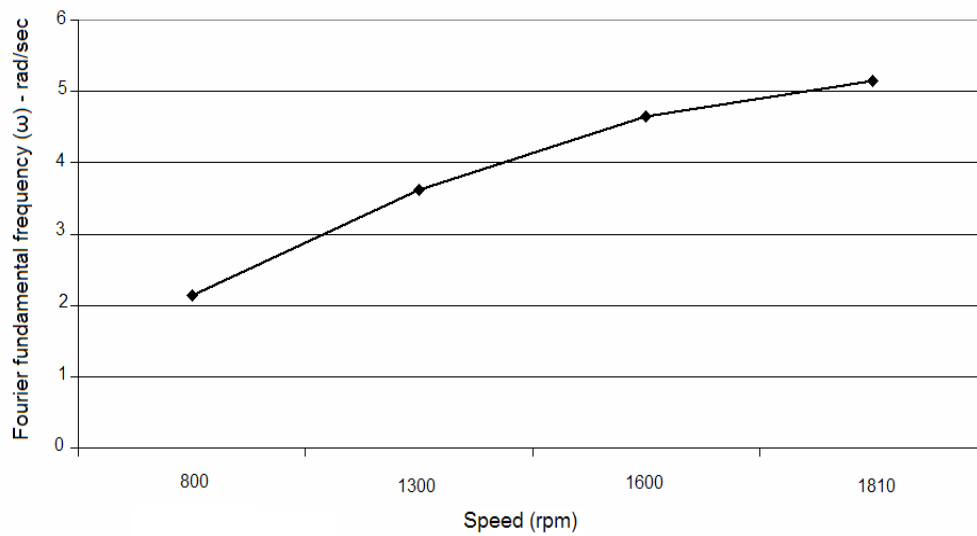


Figure (3) Accelerometer and force transducer mounting



**Figure (4) thrust force obtained during the drilling operation**  
( Speed=1300 rpm, Feed= 0.15 mm/rev, Drill diameter= 5mm, Plate thickness= 2mm )



**Figure (5) Effect of speed on  $\omega$ .**  
(Feed = 0.15mm/rev, Drill diameter = 5mm, Plate thickness = 2mm)

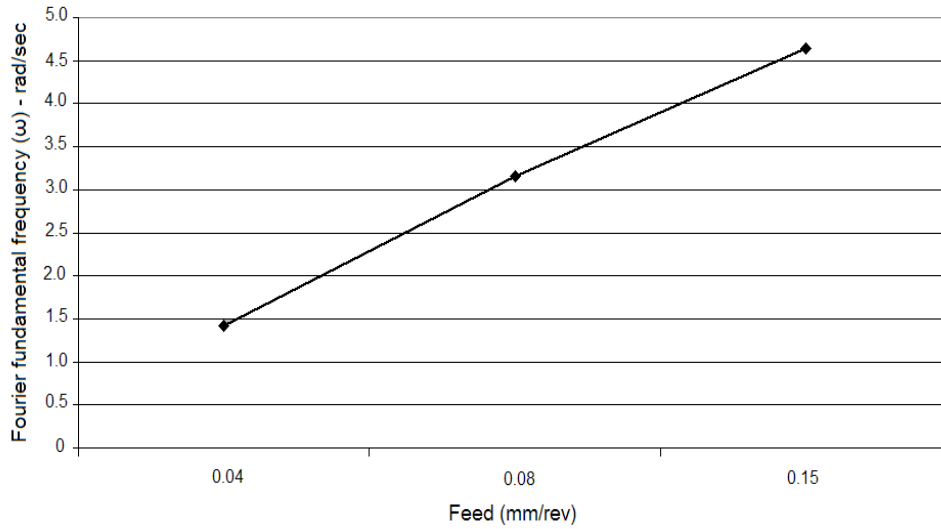


**Figure (6) Effect of feed on  $\omega$ .**

(Speed = 1600 rpm, Drill diameter = 5mm, Plate thickness = 2mm)

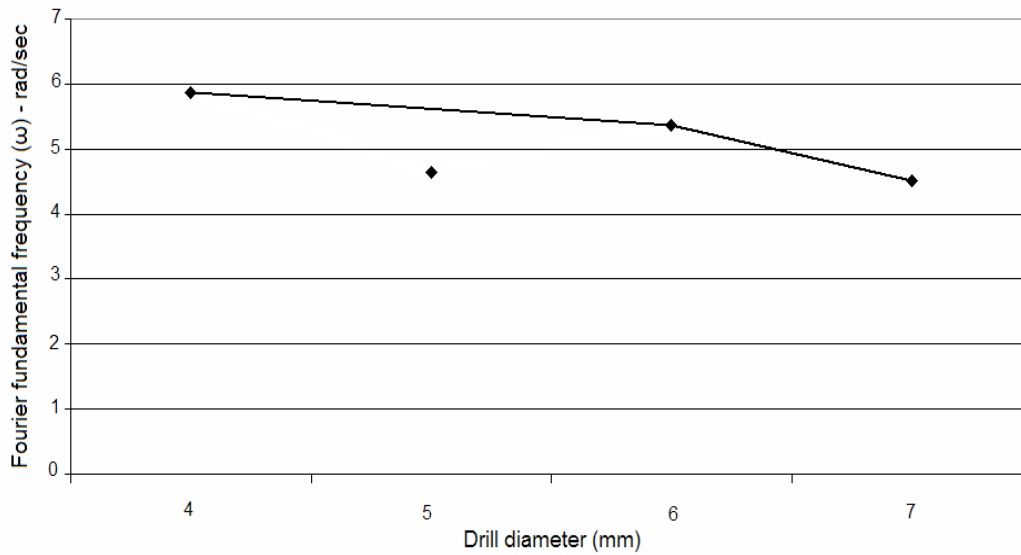


**Figure (7) Effect of drill diameter on  $\omega$ .**

(Speed = 1600 rpm, Feed = 0.15mm/rev, Plate thickness = 2mm)

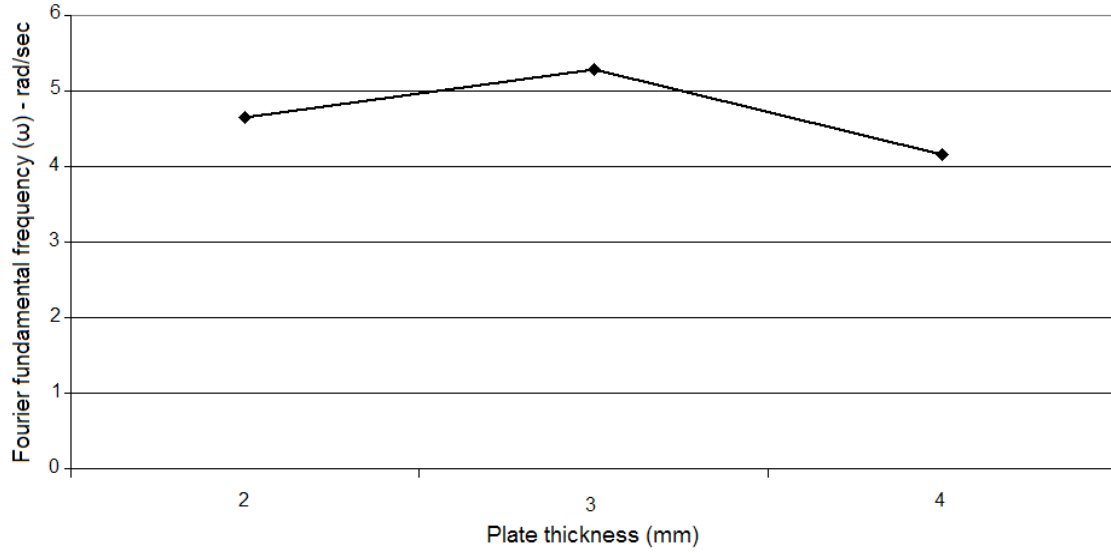


**Figure (8) Effect of plate thickness on  $\omega$ .**

(Speed = 1600 rpm, Feed = 0.15mm/rev, Drill diameter = 5mm)

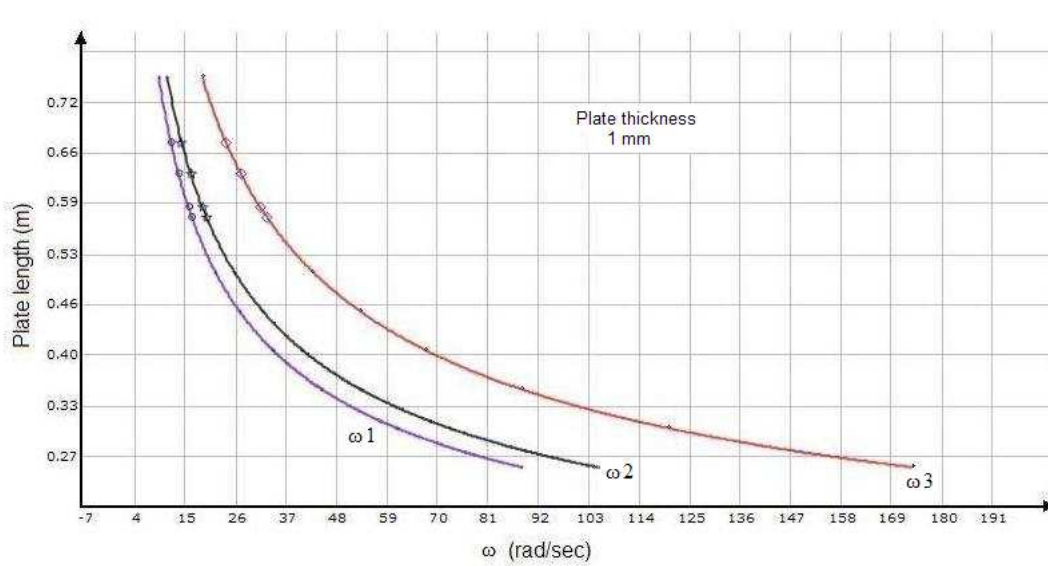


**Figure (9) First three resonance limit for CFCF plate.**

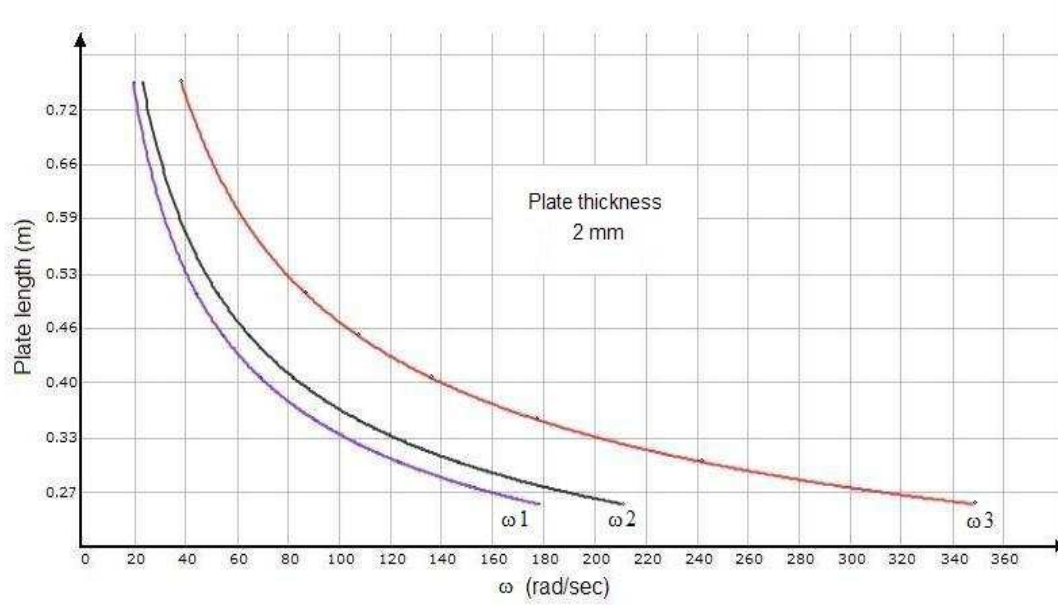


Figure (10) First three resonance limit for CFCF plate.

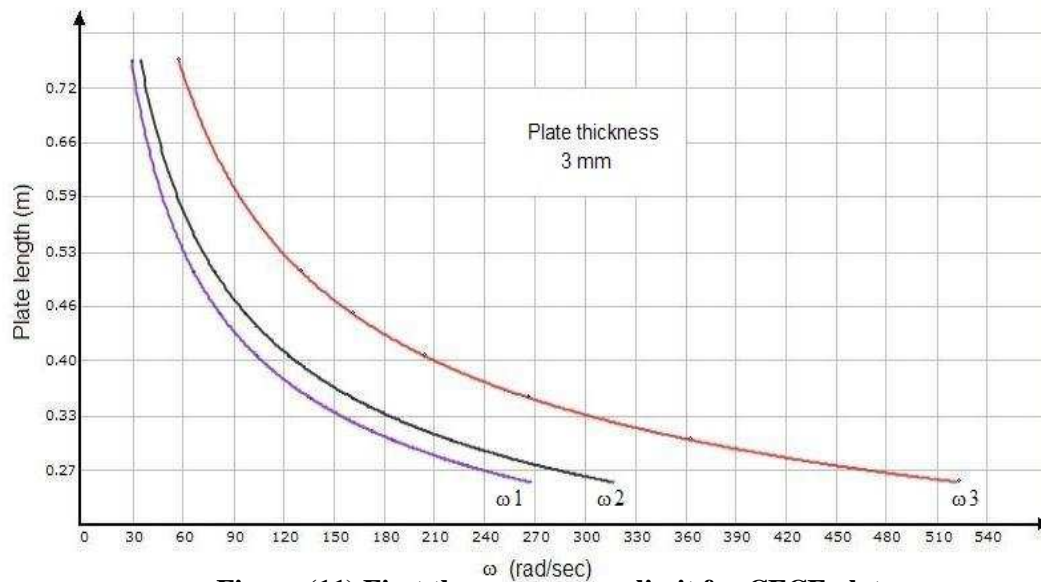


Figure (11) First three resonance limit for CFCF plate.